DOI: ADD DOINUMBER HERE

Optimal Topology of a Small-Scale Airship: a Study in Virtual Environment

Carlo E.D. Riboldi[⋆†]*, Marco Belan*[⋆]*, Raffaello Terenzi*[⋆] *and Qian Zhao*[⋆]
[⋆]*Department of Aerospace Science and Technology, Politecnico di Milano*
via La Masa 34, 20156 Milano - Italy
carlo.riboldi@polimi.it · marco.belan@polimi.it · raffaello.terenzi@polimi.it · qian.zhao@polimi.it
[†]Corresponding author

Abstract

Among the assumptions made at the lofting stage of the airship design process which may have an effect on flight performance, this paper investigates in particular those bound to the airship envelope. In order to isolate the effect of *geometry* from that of *sizing*, a suitable parameterization is introduced, allowing to investigate broadly the characteristics of a tear-drop shape. Correspondingly, a family of suitable geometries is introduced first, through a numerical procedure which allows to keep integral quantities like the wet surface and volume of the envelope at a constant value, thus ensuring that a difference in the shape (i.e. geometry) only is achieved. Next, inertia and buoyancy characteristics are computed for each geometry, assuring a similarity with respect to a baseline across all the family. With these geometrical and inertial data, a dynamic model is prepared in the flight dynamic simulation code `SILCROAD`, which incorporates a mid-fidelity aerodynamic algorithm accounting for the specific topology and sizing of the envelope and shape. Flight performance analyses in cruise-climb as well as an analysis of the free response produce results showing some trend which allow speculating on the most advantageous pick among the envelope geometries within the proposed family.

1. Introduction

When facing the design of a new airship, it is typical to run preliminary sizing algorithms such to provide engineers with values of lumped parameters, like the overall mass of the machine and its break-down into mass components, the installed thrust, or the volume of the envelope. These values are obtained so that they satisfy mission requirements (like typically carrying a certain target payload over a certain range, or for a certain time of flight, etc.), while simultaneously producing an assigned buoyancy ratio (BR),[2,12] namely the ratio of buoyancy over weight. Additional design variables may be sized at this stage of the design, especially in case the airship system is including specific thrusters which need to be sized concurrently with the rest of the machine.[7]

Almost invariably, these initial sizing procedures are based on assumptions concerning the shape of the envelope, typically obtained by composing simple solids (like half-ellipsoids, half-spheres, cylinder frustums, axial-symmetric bodies, etc.), such to produce a generally slender shape, and featuring a fineness ratio (FR) inspired by airships covering similar missions.[11]

Similarly, the sizing of the horizontal and vertical empennages is typically carried out employing statistical regressions,[2,12] based on historical data gathered from previous designs (in a similar fashion to winged aircraft[14]). These allow to assume specific values for the horizontal and vertical tail volumes, which produce areas of the horizontal and vertical empennages when the length of the envelope, hence the distance between the center of buoyancy CB and a reference point of the horizontal or vertical fins (typically the corresponding aerodynamic centers), is known.

Following the definition of a sizing solution in terms of lumped variables as just mentioned, the design comes to the detailed sizing phase, when the actual lofting of the major onboard components and their arrangement in the layout of the machine need to be specified. At this stage, the assumptions just mentioned made at the level of preliminary sizing on the envelope and empennages become constraints to be complied with. Consequently, the detailed lofting phase takes place generally too late to allow appreciating the positive or negative effects of the choice of an envelope shape or another (and similarly of a tail sizing or another) on airship performance.

The effects brought about by choosing a certain envelope shape or tail configuration and sizing are mostly visible in terms of trimmed performance and eigendynamics, which albeit often seen as secondary targets for design (when compared to the satisfaction of primary mission goals, like carrying a certain payload or ensuring a certain time of

flight), turn out to be very relevant especially for unmanned machines operating in the lower, strongly remixed layers of the atmosphere, where intrinsic stability and handling features play a significant role.

To the aim of providing a better insight into the effect of configurational choices on airship performance, a previous investigation focused on the layout of the thrusters on board,[8] presenting results clearly showing the greater effectiveness on the controlled response of the airship attainable through their specific number and positioning in the airship configuration. Conversely, the present paper aims at analyzing primarily the effect of the envelope shape.

In order to isolate the effect of the shape of the envelope from those of other characteristics of the airship, the analysis has been carried out by firstly selecting a reference shape which can be parameterized while preserving relevant properties like the center of buoyancy (CB), center of gravity (CG), volume (V_h) and wet surface (S_h) of the envelope. Failing to follow this approach would produce performance results partly due to an alteration of the envelope shape, but partly also to an alteration of other properties, making for a more complicated and potentially unfair comparison.

After selecting a suitable parameterization of the envelope, a family of envelope shape solutions such to satisfy the same preliminary sizing constraints has been defined. According to this strategy, all shapes under study will be such to comply with the specifications coming from the preliminary sizing phase (i.e. in particular a certain volume and surface), thus being in principle all feasible solutions to a same preliminary design problem. Furthermore, care has been taken to keep the rest of the design parameters constant to the maximum extent possible, especially by playing with balance masses in such a way to preserve the center of gravity position and the key components of the inertia tensor across the different candidate design solutions.

In order to capture the effect of a specific geometry on the trimmed performance and on the dynamic response of the airship, a flight dynamics model of the latter is strictly required. The mid-fidelity simulation library `SILCROAD`[13] has been employed, where methods for the simulation of the aerodynamic behavior of the envelope based on its actual geometry, as well as functions for the computations of forces acting on the horizontal and vertical tails, are available. An accurate definition of the mass/inertia and buoyancy characteristics of the airship assembly is similarly allowed.

The narration of this paper reflects the approach to a performance analysis just outlined, by firstly introducing a family of airship envelope shapes suitable for the required parameterization. The process envisaged to set up a complete aerodynamic and inertial property set for each proposed shape, yielding a complete design solution, is documented. The key points in the simulation methodology, required to allow for the performance analysis at hand to be carried out with sound accuracy, are outlined as well, briefly describing the implementation provided in `SILCROAD`. Finally, an analysis of the trimmed and dynamic performance corresponding to the family of envelopes just introduced is carried out, supporting some conclusions which allow to down-select more or less promising shapes among those considered in the analysis.

2. Design Point and Parameterization of the Envelope Shape

As explained in the introduction, the focus of the analysis presented in this paper is on the study of the effect of different shapes of the envelope on static (i.e. trimmed) and dynamic equilibrium performance. In order to isolate the effects of the shape of the envelope on airship flight mechanics performance, the following considerations need to be taken into account:

- In static trim, the drag force acting on the airship is a function (among other parameters) of the wet surface of the envelope, S_h. In forward flight, similar to aircraft, the drag force is compensated for by thrust. In climb or descent, the interplay between drag, thrust and (for airships) buoyancy produces a certain climb or descent performance. The power required for the motion, associated with drag force, is therefore compensated by thrust. The higher the drag, the higher the energy expenditure required to carry out the same mission. The shape of the airship, encapsulated in the drag coefficient, yields an influence on drag. However, the overall geometrical size of the envelope, and specifically its wet surface S_h, do have a direct effect on drag as well. In order to decouple the two effects - namely one due to the *shape* and the other due to the *absolute size* of the envelope - it is required to work with sizing solutions featuring different geometries, but an equal surface S_h.

- The buoyancy ratio $BR = \frac{B}{W}$, representing the ratio of the buoyancy B over the overall weight W of the airship, is generally a design parameter set by the designer, and specifically constant for low-altitude blimp designs which do not feature altitude-compensation systems (e.g. ballonets). Considering different envelope sizing solutions, it is desirable to keep this ratio at a constant value among them, to avoid an alteration of the share of the weight-lifting capacity between buoyancy and aerodynamic lift (from either the envelope or tails), which would influence the equilibrium solution alongside the shape of the envelope itself, thus polluting the analysis of the impact of the envelope on performance.

- Similar to the buoyancy ratio (previous point), the mutual positioning of the center of gravity (CG) and center of buoyancy (CB) has a direct effect in defining the trimmed solution, either in forward flight or climb/descent. Furthermore, it has a direct effect on pendulum, the only oscillatory mode in the longitudinal domain featured in the free response of most airships. Therefore, in order to isolate the effect of the envelope shape on the solutions just mentioned, the positioning of these two point should be kept fixed when exploring different envelope shape solutions. It should be noted that for a homogeneous envelope, typical when a blimp is considered, since no ballonets nor internal structures are considered in the design, the center of volume, center of buoyancy and center of gravity are typically coincident, when considering the envelope alone (where on the other hand, the CG and CB of the entire airship are generally non-coincident, and different from those of the envelope alone).

Considering the listing of criteria just introduced, it should be observed that finding a parameterization of the envelope shape capable in principle to cope simultaneously with all the drivers above is not trivial. For an assigned preliminary design solution, the overall weight W of the airship is assigned. This in turns yields a constant volume V_h, through the assignment of a constant buoyancy ratio BR. Therefore, looking at the first two requirements in the listing above, a constant external surface and envelope volume are simultaneously required for every specific assignment of the parameterization.

The meaning of these conditions can be better visualized by considering the ratio of the volume over the surface, which should be constant as well when both ratioed parameters are assumed constant. It is easy to note that, for example, for a sphere or an ellipsoid this ratio is not constant by definition, being conversely a function of the absolute sizing (for a sphere, as an instance, this ratio is $\frac{V_h}{S_h} = \frac{\frac{4}{3}\pi r^3}{4\pi r^2} = \frac{r}{3}$, i.e. a function of the radius r). Therefore, such solids, for example, cannot be considered for the present analysis.

Where these conditions rule out from the start many of the easiest parameterizations employed in practice, which do not offer the required flexibility to change the absolute sizing while keeping all three values in the listing above constant, on the other hand, richer parameterizations indeed exist such to allow capturing this result.

One such parameterization is constituted by a suitable polynomial, which when correctly set up allows to produce a teardrop shape. A practical realization of this approach is constituted by the Lotte airship, a prototype extensively employed for setting up a case-study on many points related to airship design and characterization.[4,5] For that airship, the radius r of the axial-symmetric envelope has been assigned as an explicit homogeneous function of the nondimensional abscissa $\zeta = \frac{x}{L_h}$ according to the following Eq. (1)

$$r(\zeta) = L_h \sqrt{\sum_{i=1}^{N} a_i \zeta^i}, \tag{1}$$

where L_h is the length of the envelope, x increases from zero on the forward tip of the envelope to L_h at the back tip, and a_i are the coefficients of the polynomial. Specifically, for the Lotte case a homogeneous 7-th order polynomial has been considered (i.e. with $N = 7$). The yellow sketch in Fig. 1 displays the result of this parameterization in the specific case of the Lotte airship.

Observing the teardrop shape qualitatively, it is noteworthy how it is sufficiently flexible to allow exploring different shapes while simultaneously satisfying all three requirements mentioned previously, by for instance increasing the top radius. However, as known, the management of a polynomial shape function so as to carry out a parameterized analysis is not trivial. In practical terms, considering to start from a reference condition where L_h and the coefficients a_i are known, and assuming to set a new value of the top radius r_M to be achieved (either higher or lower than the current reference value), what is required would be to act on L_h and the a_i coefficients, changing them towards that goal, while simultaneously keeping the external surface and volume, as well as the position of the center of buoyancy (non-dimensional) constant. While theoretically straightforward, due to the nature of the polynomial shape function this problem turns out extremely hard to manage in practice. Actually, a small change in the coefficients produces a potentially very intense change in the shape, which may easily result in an abrupt and complete departure from the desired teardrop shape.

In order to overcome the limitations of a parameterization approach through a polynomial function, the teardrop shape has been reproduced according to a different function describing the radius. The forward part of the envelope, extending from the forward tip (corresponding to $x = 0$) to an abscissa x_{P_1}, is described via an ellipsis, centered on the longitudinal axis at x_C and featuring semi-axes a (major) and b. From the position of x_{P_1} to the back tip of the envelope $x_T = L_h$ the radius is described by a piecewise-cubic spline interpolation of three points (i.e. two cubic elements), namely (x_{P_1}, r_{P_1}), an additional intermediate point (x_{P_2}, r_{P_2}) such that $x_{P_1} \leq x_{P_2} \leq x_T$, and the back tip point $(x_T, 0)$. In order to ensure a suitable regularity of the so-defined shape function, the derivative of the radius $\frac{\partial r}{\partial x}\Big|_{x_{P_1}}$ is constrained to be equal on both sides, and the slope of the spline interpolation at the tip $\frac{\partial r}{\partial x}\Big|_{x_T}$ is similarly constrained to keep below a threshold. In analytic terms, the new ellipsis-cubic spline representation can be posed as in Eq. (2),

$$
\begin{aligned}
r(x) &= \begin{cases} \dfrac{b}{x_C}\sqrt{2xx_C - x^2}, & 0 \le x \le x_{P_1} \\ P^3(x), & x_{P_1} < x \le x_T \end{cases} \\
s.t.: \; c_1 &: \frac{b}{x_C}\frac{x_C - x_{P_1}}{\sqrt{2x_{P_1}x_C - x_{P_1}^2}} = \left.\frac{\partial P^3(x)}{\partial x}\right|_{x_{P_1}} \\
c_2 &: \left.\frac{\partial P^3(x)}{\partial x}\right|_{x_T} = \tilde{d} < 0
\end{aligned}
\tag{2}
$$

In Eq. (2), $P^3(x)$ represents a piecewise-cubic interpolating function based on three nodes (i.e. two cubic elements). Condition c_1 imposes the equality of the derivatives of the elliptic and piecewise-cubic components of the shape function at the merging points (x_{P_1}, r_{P_1}), whereas condition c_2 imposes a negative derivative of the piecewise-cubic interpolating function at the tail tip x_T, further bounding its value under the (negative) threshold $\tilde{d}$.

Before attempting to generate a family of envelope profiles with this newly proposed shape function, by changing the top radius and computing the corresponding parameters defining the shape, a procedure to automatically compute the parameters fitting the shape function to an assigned absolute geometry has been tested on the original Lotte case. The result is presented in Fig. 1, allowing a comparison with respect to the original envelope obtained with a 7-th order polynomial. It can be observed how the new parameterization (sketched in blue) yields an accurately comparable result with respect to the original polynomial parameterization (yellow).

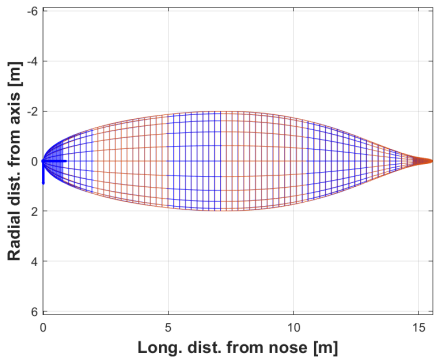

Figure 1: Teardrop shape of the Lotte airship, as obtained with a 7-th order polynomial (yellow) and the new proposed shape function based on an ellipsis and a two-elements cubic spline (blue).

The numerical procedure implemented to bear this result is essentially that of a constrained best-fit. The parameters demanded to the fitting algorithm for automatic tuning can be wrapped in the array $\boldsymbol{p}$ in Eq. (3)

$$
\boldsymbol{p} = \left\{ x_C, b, x_{P_1}, x_{P_2}, r_{P_2}, x_T, \left.\frac{\partial r}{\partial x}\right|_{x_T} \right\}. \tag{3}
$$

Notably, the parameters in $\boldsymbol{p}$ correspond to the set of data required to assign a specific geometrical shape based on the parameterization of the envelope just introduced in Eq. (2). The norm to be minimized by the fitting algorithm is defined as a quadratic norm of the difference between the evaluation of the ellipsis-cubic spline parameterization and the 7-th order polynomial (Eq. (1)) on an arbitrarily refined grid between $x = 0$ and $x = x_T$. This provides the fitting algorithm with a blueprint of the desired teardrop shape, thus steering the fitting process towards a physically acceptable solution. Furthermore, a set of constraints is applied, namely assigned external surface $\bar{S}_h$, volume $\bar{V}_h$, relative position of the center of buoyancy $\frac{\bar{x_{CB}}}{L_h}$, and maximum radius $\bar{r}_M$. Clearly, S_h, V_h, x_{CB} and r_M can be computed for an assigned set of the parameters $\boldsymbol{p}$ (the same is true for an assigned set of the parameters which define the 7-th order polynomial, of course). Additionally, in order to facilitate the search for a teardrop-resemblant solution, two inequality constraints are imposed on the derivatives of the shape function, yielding the analytic description of the fitting problem in Eq. (4)

$$
\begin{aligned}
&\min_{\boldsymbol{p}} J = \sum_i \left(r^{ecs}(x_i) - r^{pol}(\zeta_i) \right)^2 \\
&s.t. : e_1 : \int \mathrm{d}S = \bar{S}_h \\
&\quad e_2 : \int \mathrm{d}V = \bar{V}_h \\
&\quad e_3 : \left(\frac{1}{V_h} \int \mathrm{x} dV \right) \frac{1}{L_h} = \frac{\bar{x_{CB}}}{L_h} \\
&\quad e_4 : \max r(x) = \bar{r}_M \\
&\quad i_1 : \max \frac{\partial^2 r}{\partial x^2} \leq 0, 0 \leq x \leq x|_{r_M} \\
&\quad i_2 : \max \frac{\partial r}{\partial x} \leq 0, x|_{r_M} \leq x \leq x_T
\end{aligned}
\tag{4}
$$

In Eq. (4) r^{ecs} and r^{pol} represent the ellipsis-cubic spline and the polynomial shape functions respectively. The shape function r^{ecs} is a function of $\boldsymbol{p}$, whereas the coefficients of the polynomial function r^{pol} are assumed as those of the Lotte case. The actual radii obtained from the polynomial function however are a function of $L_h = x_T$, which is among the parameters in $\boldsymbol{p}$ (i.e. changed within the fitting algorithm). The inequality constraint i_1 imposes a convex shape of the front part of the airship contour ahead (i.e. to the front tip) of the station of the maximum radius, whereas i_2 imposes only a non-positive trend of the radius behind the same station, which corresponds to a tail shape always converging to a tail tip.

The problem stated in Eq. (4) can be solved through a gradient-based algorithm. The solution for the specific case of the reference Lotte airship (i.e. the sizing solution of that specific airship) has been already shown in Fig. 1. As anticipated, a family of envelope shapes solving the same problem, yet such that its solution be associated to a different value of the maximum radius $\bar{r}_M$, can be obtained as well. In particular, the problem has been solved satisfactorily for $\bar{r}_M$ ranging between 0.8 and 1.2 times the reference value for the Lotte airship (which is 2 m). The plots in Fig. 2 show some examples of the corresponding solutions.

It can be observed how a reduction of the target top radius from the original Lotte value produces basically a scale-down of the original geometry, with slight alterations to the original shape, mostly an increase in the tail cone radius. Conversely, when the required value of the top radius is increased, the solution tends to feature a more bulged forward component and a thick spine to the back (the latter featuring also a rather visible longitudinal span where the radius keeps stationary).

3. Fitting Inertial Characteristics and Complete Model Generation

In the previous section we introduced a shape parameterization such to produce a family of envelopes which satisfactorily comply with a set of requirements, assuring a similarity with respect to a starting airship baseline (i.e. the Lotte airship in this case). Considering in particular the listing at the beginning of the previous Section 2, the envelopes generated according to the fitting procedure described thereby comply with the first two requirements, i.e. they all feature the same external surface and volume. Furthermore, the relative positioning of the center of buoyancy over the full length of the airship is kept fixed to the value assumed from the baseline (see the equality condition e_3 in the fitting problem, Eq. (4)).

However, the third point in the initial listing of Section 2 refers to the mutual positioning of the center of gravity CG vs. the center of buoyancy CB. For an airship envelope designed for a blimp and without envisaging ballonets or other altitude-compensation systems, when the material employed for the manufacture is homogeneous, the position of the center of gravity should coincide with the center of volume and the center of buoyancy ($CG \equiv CB$). Therefore, within the family of parameterized envelopes, the center of gravity should change as much as the center of buoyancy.

In order to convert the shape of the envelope into an a dynamic model of an airship featuring a complete set of aerodynamic and inertial properties, it is firstly required to associate some mass density properties to the envelope skin and lifting gas, which are the two physical components of the envelope of a blimp. Secondly, all other components on board need to be accounted for as well, in terms of their mass, and of their positioning in the airship layout, thus yielding a contribution to the overall inertia of the airship. Such additional components are namely the horizontal and vertical empennages, which beside a certain mass distribution come with aerostatic (i.e. volume) and aerodynamic properties, and components like the motor/s, batteries and other on board systems, which are associated to mass but not to any significant aerostatic/aerodynamic property. The latter can be modeled as lumped masses.

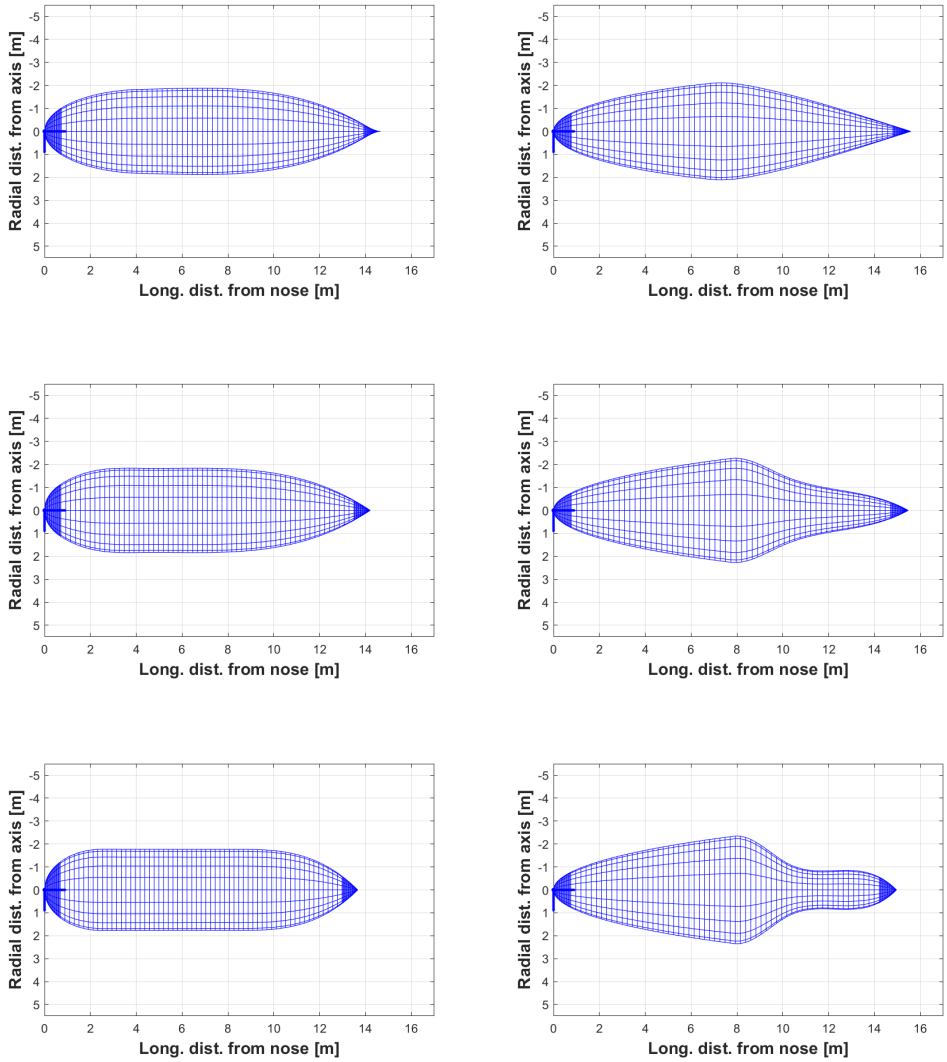

Figure 2: Examples of the geometries of envelopes within the family generated as described in Section 2. Left, from top to bottom: top radius reduced to 94%, 86% and 80% of baseline (Lotte). Right, from top to bottom: top radius increased to 106%, 114%, 120% of baseline (Lotte).

When adding further components associated to mass in addition to the envelope in the layout of an airship, the center of gravity of the resulting (complete) system will generally travel away from that of the envelope alone. Similarly, the overall volume of the system, producing buoyancy, will be slightly different from that of the envelope, in particular due to the volume of the empennages. Correspondingly, the center of buoyancy will generally be different from that of the envelope alone. To the aim of carrying out an analysis of the effect of the envelope shape on the flight mechanics performance, the effect of all other components of the system should be kept down to a minimum, in order to isolate the effect under analysis. This is embodied firstly by the third point in the listing on top of Section 2.

In order to achieve the goal of isolating as much as possible the effect of different airship envelopes on performance from all other effects, a procedure for setting up the complete dynamic model corresponding to each of the entries in the family of aerodynamically equivalent envelopes, designed as described in Section 2, has been envisaged. The major steps in this procedure are as follows.

1. *Compute envelope mass and inertia properties.* This is performed starting from the assigned geometry of the envelope, based on a thickness and material density of the envelope skin and on a density of the lifting gas. Since all envelopes share the same volume and surface, the mass of the envelope material and that of the lifting gas are employed in practice, instead of the respective densities. This allows to comply directly with the characteristics

of the outcome of the preliminary sizing phase, where global values of the envelope mass and lifting gas mass are components of the sizing output.

2. *Position the horizontal and vertical tail*. The properties of the fins are kept identical to those of the baseline airship (Lotte). Their longitudinal positioning is at the same distance to the back of the center of buoyancy of the envelope as the baseline. However, the positioning of the root section is such to comply with the actual local radius of the envelope. Notably, the sizing of the tails like in the original baseline, and their positioning at the same distance from the center of buoyancy of the envelope, produces a preservation of the tail volume (i.e. the product of the tail surface by its distance with respect to the center of buoyancy[2]) among all solutions within the family. This allows to comply with the features of the preliminary design solution, as well as to ensure a similarity in the stabilization effectiveness around the pitch and yaw axes.

3. *Position other mass components to obtain inertial similarity wrt. baseline*. This passage consists in delegating to a numerical solver the selection of the mass of four point masses, as well as the positioning of some of them in the airship topology, in order to satisfy a set of constraints. These constraints define the longitudinal and vertical position (in body coordinates) of the center of gravity CG of the airship vs. the center of buoyancy CB of the airship, the total mass of the airship, and finally the value of the three axial components (in a body reference) of the inertia tensor. All these values are steered by a solver through an update of the independent masses and positions of the point mass elements, so as to adhere to the corresponding values obtained from preliminary sizing (i.e. in the present case from the baseline Lotte airship).

The mathematical formalization of the latter point 3. in the previous procedure can be provided as follows. Let the masses m_k, $k = 1, \dots 4$ be the point masses of as many elements in the dynamic model of the airship. The problem can be configured as a least-squares fitting, where the array of parameters is assigned as $\boldsymbol{q}$ in Eq. 5

$$\boldsymbol{q} = \{m_1, m_2, m_3, m_4, x_{m_1}, x_{m_4}, z_{m_4}\}, \tag{5}$$

wherein the longitudinal position of the first and fourth masses x_{m_1}, x_{m_4}, and the transverse position of the fourth mass z_{m_4} are parameters to be set. Conversely, the other positions are set as follows:

- z_{m_1} is set such that the point mass m_1 be on the contour of the envelope (similar to a nacelle),
- (x_{m_2}, z_{m_2}) correspond to the envelope front tip position, so that m_2 is located on the nose of the airship,
- (x_{m_3}, z_{m_3}) correspond to the back tip of the envelope, so that m_3 is located on the back tip of the airship.

The array of residuals to be targeted in the least-squares fitting problem, in accordance with point 3. in the previous listing, is reported in Eq. 6,

$$\begin{aligned} s_1 &= x_{CG} - x_{CB} + \Delta^{\text{bl}}_{x_{CG-CB}} \\ s_2 &= z_{CG} - z_{CB} + \Delta^{\text{bl}}_{z_{CG-CB}} \\ s_3 &= J_{CG,xx} - J^{\text{bl}}_{CG,xx} \\ s_4 &= J_{CG,yy} - J^{\text{bl}}_{CG,yy} \\ s_5 &= J_{CG,zz} - J^{\text{bl}}_{CG,zz} \\ s_6 &= m - m^{\text{bl}} \end{aligned} \tag{6}$$

where superscript $(\cdot)^{\text{bl}}$ stands for baseline, $\Delta_{x_{CG-CB}}$ and $\Delta_{z_{CG-CB}}$ represent assigned biases between the CG and CB in the longitudinal and vertical (body) directions respectively, J_{CG} represents the components of the inertia tensor of the airship in a body reference, and m the mass of the airship. Finally the least-squares problem can be set-up according to the following Eq. (7)

$$\min_{\boldsymbol{q}} \sum_{j=1}^{6} s_j^2, \tag{7}$$

which can be solved numerically, provided a method is available to compute the volume, mass and inertia features of the airship, required to populate the expressions of the residuals in Eq. 6. Within the present study, an object-oriented Matlab® library developed at the Department of Aerospace Science and Technology of Politecnico di Milano, named `AFL` (an acronym for *A*ssembly *F*eatures *L*ibrary), has been employed. A major advantage of operating in Matlab® environment is the chance to employ proven and efficient built-in methods for managing optimal problems,

which allow for a unified numerical treatment of the entire process encompassing firstly the computation of a new envelope geometry within the family of envelopes of interest (starting from a baseline like the Lotte), as described in Section 2, and secondly the setup of a corresponding inertial model, according to the fitting process of inertial properties just described in the present section. The `AFL` library bridges the gap between the definition of an airship topology, completed by mass density properties for extended bodies and by masses for lumped mass components, and the computation of buoyancy and inertia properties (including the position of the CG and CB, as well as the overall buoyant volume, mass and inertia tensor components with respect to an arbitrary point or reference) required for assigning a dynamic model. Thanks to the fact that `AFL` is natively and entirely written in Matlab® environment, the computation of the inertial and volumetric properties takes place without the need to invoke a CAD representation software or any other external routine for the task, thus additionally streamlining the numerical implementation of the synthesis of dynamic models corresponding to each geometry and topology within the family.

It is noteworthy that the best fit problem in Eq. (7) is such that when all s_j in Eq. (6) are null, an inertia- and buoyancy-equivalent solution is obtained with respect to the baseline. However, in practice this result is never strictly achieved. The residuals registering the most significant discrepancy are s_3, s_4 and s_5, where an error of some percent unit with respect to the baseline is in order.

Figure 3 displays some examples of the inertia and volume model of airships from `AFL`, corresponding to some of the entries in the family of envelopes of interest, showing the actual three-dimensional representation of the envelope and tails, as well as the positioning of the point masses on board, four of which have been positioned/tuned according to the procedure introduced in the present chapter. Notably, mass m_1 is generally positioned very close to m_2 close to the front tip (making it unapparent in the sketches), whereas mass m_4, left free to range potentially also within the radius of the envelope, is placed by the fitting algorithm on the envelope skin.

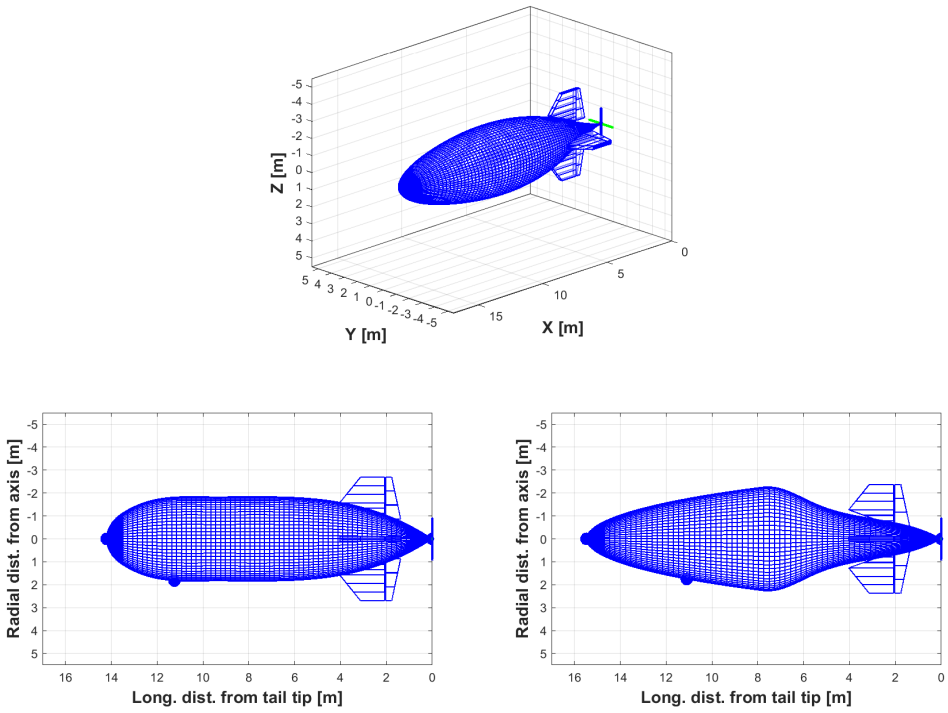

Figure 3: Example volume and inertia models obtained as an outcome of the overall model setup problem described in Sections 2 and 3, employing `AFL`. Top plot: three-quarter view of baseline (Lotte). Left plot: top radius 86% wrt. baseline. Right plot: top radius 114% wrt. baseline.

This graphical representation is among the outputs of the `AFL` software, whereas as said the numerical values of the position of the CG and CB, the buoyant volume V (which is due to both the envelope volume V_h and that of the tails), the mass m and the components of the inertia tensor J_{CB} of the airship in a body reference centered in the CB are available for each of the solutions. In the present study, the sizing of the fins has been set according to the baseline geometry of the Lotte airship, and left unchanged except for a rigid translation as explained at point 2. in the procedure for the setup of a dynamic model. Consequently, some discrepancy between the local slope of the envelope and the matching (i.e. inner) face of the fin is encountered, as visible in the bottom sketches in Fig. 3.

4. Dynamic Model

In order to carry out an analysis of the trimmed performance of the airship, as well as of the free response of the system, for different entries in the family of airships under study, a complete dynamic model has been setup for each of them. The model has been setup employing SILCROAD, an object-oriented flight dynamics simulation library already validated and employed for aircraft and airship simulation.[9,10,13]

The basic features of this model include the allowance for an arbitrary definition of the reference point for writing the equations of motion of the flying craft, an accurate definition of the position of the *CG*, *CB*, of the volume, mass, and inertia tensor (fully-populated), and for the accurate positioning on board of an unlimited number of fins and thrusters (with arbitrary orientations). For thrusters, a thrust model allows to modulate the intensity of each thrust vector with respect to a throttle control variable, as well as a function of velocity (or Mach) and altitude. For fins, each come with a deflectable trailing edge surface, which allows for a corresponding aerodynamic control.

For the airship model, SILCROAD allows to either specify stability and control derivatives, or conversely to provide the input required to setup an aerodynamic model as described by Munk-Jones-DeLaurier theory[3,6] for the envelope part. In essence, the actual shape of the envelope can be specified by the user, and a discretization of the airship volume along the longitudinal axis is carried out. For each discrete element, a method for computing three local contributions to aerodynamic force values and the corresponding contributions to moment is implemented.[3] For this computation, the method accounts for the local value of the airspeed vector, itself due to the linear velocity and rotational rate of the body, and to the local acceleration vector.[1,3] The aerodynamic model estimates the drag according to an attached flow and a cross-flow effect,[3] thus allowing to effectively capture the behavior of the airship also for rather high angles of attack,[4] which might be encountered on an airship more easily than on a winged aircraft, for instance when maneuvering in near-hover conditions.[9] The contribution of the envelope to the overall aerodynamic actions on the airship is extended from the nose to a longitudinal station defined by the user in proximity of the leading edge of the root airfoil of the tails.

Provision is made for specifying three axial components of apparent inertia, which in the present study are estimated by employing closed-form expressions available for axial-symmetric ellipsoids, where the two semi-axis have been chosen based on the length of the airship (major semi-axis) and top radius of the envelope (minor semi-axis).

The fins are treated according to a lumped model, where lift, drag and moment coefficient sensitivities specified as known parameters are employed to compute aerodynamic forces and torque due to attached flow and cross-flow components,[3] and the knowledge of the positions of the aerodynamic center and cross-flow force center allow to compute the overall moment due to the aerodynamic forces.

Figure 4 displays two representations of the complete dynamic model corresponding to the same entries in the family of airships employed for Fig. 3, as obtained from SILCROAD. Notably each fin is represented by a rectangular shape, which is only representative of the area of the fin and its span, and irrespective of the actual planform. This is in line with the aerodynamic modeling adopted for the fins, as well as with the fact that the inertia of the airship is specified by the user and not computed internally. Also displayed are the *CG* and *CB* of the airship, the position of the only thruster (where the thrust force is acting), the positions of the aerodynamic center and cross-flow center of each fin, and the hinge lines of the aerodynamic surfaces. The chin lines along the envelope indicate the longitudinal range of application of the aerodynamic model for the envelope (i.e. out of this range the envelope does not contribute to aerodynamic forces and moments).

The aerodynamic model implemented in SILCROAD has been validated extensively with respect to wind tunnel data on the Lotte airship, with negligible errors on both force and moments recorded in static trials on a range between [-30,30] deg of the angle of attack.

5. Analysis of Flight Performance and Dynamics

By employing the dynamic model of each of the airships in the family introduced in the previous sections, it is possible to carry out performance analyses which should tell whether a specific shape of the envelope is advantageous with respect to another. The metric considered in this work is two-fold. Primarily, an analysis of static flight performance is carried out, where the cruise-climb flight envelope of the airship is computed. Secondly, the free response of the system is computed, employing linear analysis and the computation of the eigenvalues in the longitudinal and lateral directional domains.

The cruise-climb flight envelope of the machine, similar to a winged aircraft, can be practically obtained from static trim analyses, and allows to capture the top performance attainable by an airship in static equilibrium. The plots in Fig. 5 display comparisons of the flight envelopes of two couples of airships. The left plot displays a comparison between the reference (Lotte) and the smallest top radius geometry within the family, whereas the right plot refers to the same reference and the largest top radius geometry.

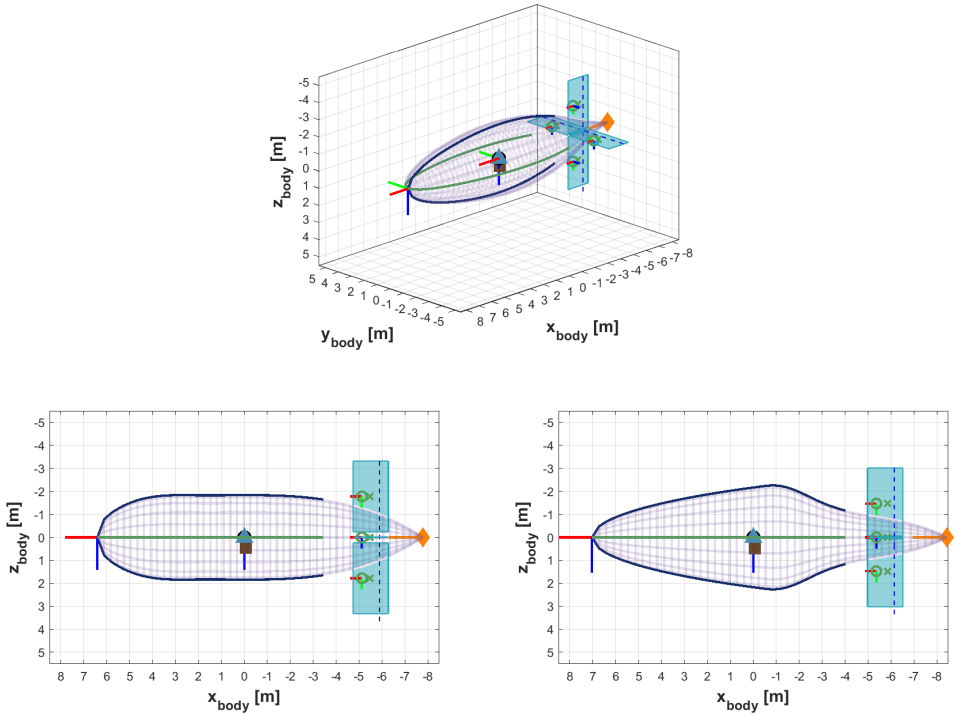

Figure 4: Representation of the main aerodynamic characteristics (envelope, fins) and reference points from the dynamic model built in `SILCROAD`, for the same entries in the airship family of Fig. 3. Brown square: airship *CG*. Blue triangle: airship *CB*. Green circle: aerodynamic center of fin. Green cross: cross-flow force center of fin. Amber diamond: position of thrust vector (motor). Blue circle: reference point for writing dynamic equations (*CB* in this case).

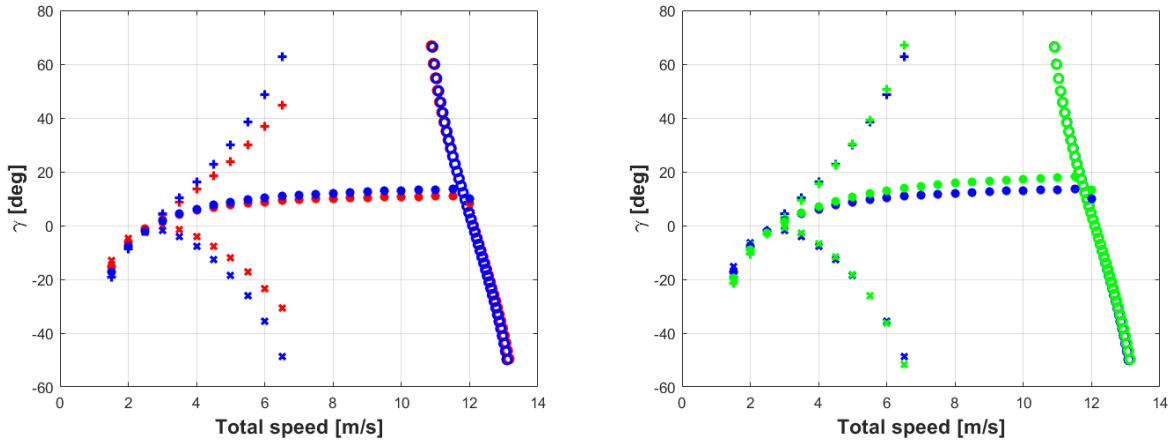

Figure 5: Comparison of static cruise-climb flight envelopes. Left plot: baseline (blue) vs. 80%-of-baseline top radius airship (red). Right plot: baseline (blue) vs. 120%-of-baseline top radius airship (green). Crosses/pluses: climb rate with ±25 deg elevator deflection. Dots: climb rate with null elevator deflection. Circles: velocity and climb angle at full power.

In these plots, the mostly-vertical line to the right has been obtained trimming the airship at full power, thus representing the maximum velocity attainable in static equilibrium in horizontal flight, climb or descent. The two lines to the left of the plot correspond to equilibrium conditions at increasing total velocity values (i.e. an increasing imposed modulus of velocity), with an assigned deflection of the elevator to the positive and negative stroke-end of the actuators, corresponding to ± 25 deg.

Interestingly, the difference between the maximum velocity attained at full power is negligible, even considering the most extreme geometries in the family of airships under study. This is a direct result of the equality in the overall wet surface of all machines considered, as well as a similarity in the balance attained through similarly positioned CG and CB for all machines, which makes the aerodynamic loading of the tails required for trim (hence the corresponding drag) similar in all cases. On the other hand, much more pronounced differences are found on the climb and descent lines at increasing speed. In particular, the climb and descent speed are significantly reduced (in modulus) by a change in the geometry towards a smaller top radius (left plot). Conversely, the top climb/descent performances are less different from the baseline in case the geometry corresponding to the top radius is considered (right plot), but a more marked difference is encountered in this case for a null value of the elevator deflection.

Figure 6 displays the behavior with respect to the reference case of the climb and descent angles attained for ± 25 deg and null deflection of the elevator, for a total velocity (modulus) of 6 m/s. The reduced climb performance associated with the lowest radii is apparent. This can be associated mostly to a different distribution of aerodynamic loads locally on the envelope, contributing to an overall different system of aerodynamic force and moment acting on the airship. Correspondingly, geometries with a higher top radius within the family tend to be associated to a slightly advantageous trim performance in positive and negative climb performance.

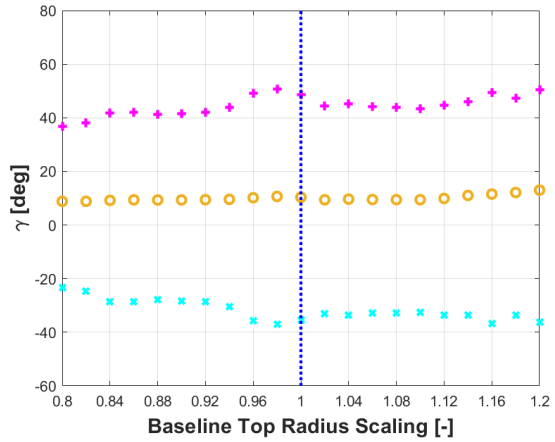

Figure 6: Comparison of maximum static climb/descent angle for an assigned trim velocity modulus of 6 m/s and an elevator deflection of ± 25 deg, considering all airships in the family. Cyan crosses: climb angle with +25 deg elevator deflection. Magenta pluses: climb angle with -25 deg elevator deflection. Yellow circles: climb angle with zero elevator deflection.

As a general comment, looking at the specific geometries associated to a growing number of the top radius considered in this study, the higher the top radius, the more pronounced the appearance of a bulged forward part and a tail spine. Conversely, very low top radius values are associated to an almost uniform, almost-cylindrical shape of the envelope. Therefore, it appears that the former shape, associated to a higher top radius, is generally such to provide homogeneously better climb performance than a more cylindrical one.

It should be remarked that the sizing solutions are the result of numerical fitting procedures, which do not bear a perfect result on all parameters. In particular, numerical slight violations of the constraints in the fitting problems in Eq. (4) and (7) may be present. However, these have been checked to be practically negligible, therefore they are not such to invalidate the speculation just introduced.

An analysis of the free response can be carried out on a linearized model of the airship, obtained taking as a reference point a static trimmed condition in forward flight (as typical for winged aircraft as well). The computation of a linearized model from the fully non-linear dynamic model built with `SILCROAD` is carried out via methods available within the library, which implement a perturbation approach to compute the sensitivity of aerodynamic forces and moments to state and controls and for thrust, whereas the contributions of gravity and buoyancy within the matrices of the linearized system are computed explicitly from analytically-linearized expressions.

Figure 7 displays a comparison of the longitudinal (left plot) and lateral-directional eigenmodes of the system, considering all airships within the family in a same reference trim condition at 6 m/s in horizontal flight.

Considering the map of longitudinal eigenmodes, a significant difference is encountered on the pendulum mode. Interestingly, this is mostly felt on the damping of this mode, which is decreased for increasingly large values of the top radius, to the point that for the most extremely large values instability is reached. The pendulum mode is generally influenced by the mutual positioning of CB and CG, and by the damping effect induced by the horizontal

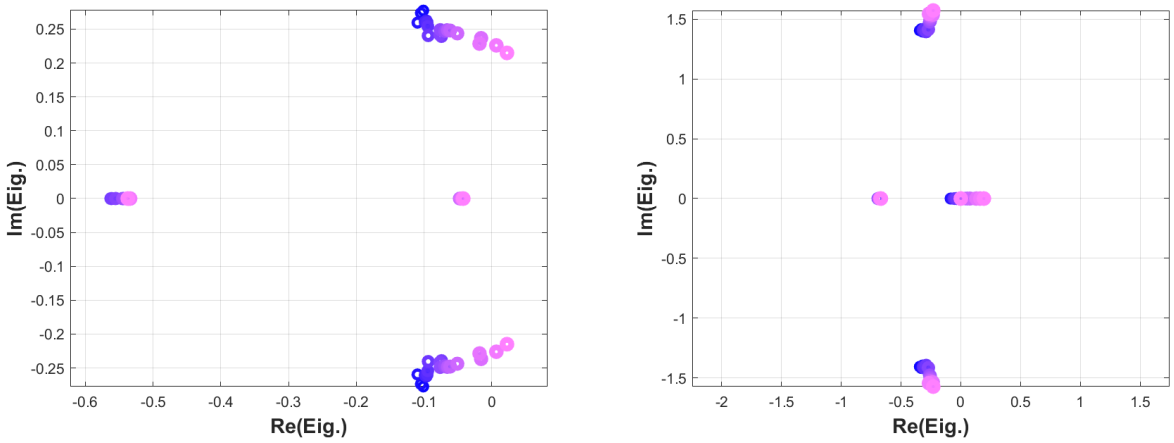

Figure 7: Comparison of the eigenmodes obtained considering a trimmed horizontal flight condition at 6 m/s, for all airships in the family. Left plot: longitudinal dynamics. Right plot: lateral-directional dynamics. Blue to magenta: from 80% to 120% of baseline top radius.

tail. Conversely, in this study good care has been taken specifically to avoid differences in these characteristics, across different geometries in the family. Therefore, the significant difference encountered in the damping of the pendulum can be imputed to the different behavior of aerodynamics around the airship envelope, resulting from a different geometry of the latter.

Of course, as pointed out also for the cruise-climb flight envelope analysis, since the inertia fitting problem (see Section 3) is not solved exactly but according to a least-squares approach, residuals in the components of the inertia tensor, including the pitching component, may be non-null. Therefore, additional polluting effects shall result from such difference as well. However, a rather marked pattern can be recognized in Fig. 7 which supports the existence of a trend in dynamic performance in association with geometrical differences.

Considering the lateral-directional domain, the difference between the considered solutions on the poorly damped roll mode is mostly associated to the slightly changed radial positioning of the tails, such to cope with the local radius of the envelope on the tail cone. This implies a difference in aerodynamics and in roll inertia, which can be only partially recovered by fitting the tuning parameters in Eq. (7), i.e. the identities and positions of the point masses. Interestingly, the side-slip subsidence mode (real) turns increasingly less stable, then definitely unstable, for increasing values of the top radius and the corresponding geometries.

Therefore, it can be generally argued that the geometries corresponding to increasing values of the top radius, featuring a bulged forward part and a prominent tail spine, tend to be associated to a markedly decreasingly-stable behavior of pendulum and side-slip subsidence eigenmodes.

6. Conclusions

The focus of this analysis has been put on the effect of the envelope shape of an airship on static and dynamic flight performance. To the aim of isolating this effect from others bound to sizing, and potentially due to a different value of the wet surface, lifting volume, positioning of the center of buoyancy relative to the length, as well as to inertial factors like the mutual positioning of the center of gravity with respect to the center of buoyancy, the problem of introducing a parameterization allowing to generate geometries equivalent as much as possible under these criteria has been faced first. Secondly, an inertial and volumetric equivalence has been seized by setting up purpose-defined fitting problems.

On a family of airships featuring virtually identical wet surface, volume, mutual positioning of the center of gravity and buoyancy, plus the same mass and key components of the inertia tensor, a parameterized flight performance analysis has been carried out. The entries in this family feature increasing values of the top radius. The cruise-climb envelope has been computed, showing that a smaller top radius, and the very regular corresponding geometry, is generally associated to a more modest climb performance. Conversely, the latter is not significantly impacted for higher values of the top radius, which correspond to a geometry featuring a prominent bulged part and a tail spine.

Finally, an analysis of the longitudinal and lateral directional eigenmodes performed on all airships within the family has revealed a significant sensitivity of the pendulum mode and of side-slip subsidence to the geometries at hand. In particular, the damping of the oscillatory pendulum mode is decreased, and similarly both that mode and

the real side-slip subsidence mode appear to travel towards instability when considering geometries corresponding to higher top values of the radius. These are associated again to a more pronounced forward bulge and a visible tail spine.

Considered together, these analyses tend to suggest that where a more regular, almost cylindrical shape is advisable for a generally more naturally stable free response (both in the longitudinal and lateral-directional domains), a better static flight performance may be associated to a higher top-radius and a generally less regular geometry, featuring a prominent maximum of the radius in its profile.

7. Acknowledgments

This project has received funding from the European Union under grant agreement No.101098900, within the European Innovation Council (EIC) Pathfinder Open programme of 2022 (call HORIZON EIC 2022 PATHFINDEROPEN 01).

References

[1] H. Bateman. The inertial coefficients of an airship in frictionless fluid. Technical report, NACA, 1924. National Advisory Committee for Aeronautics, Report No.164.

[2] G. E. Carichner and L. M. Nicolai. *Fundamentals of Aircraft and Airship Design*. AIAA Education Series. American Institute of Aeronautics and Astronautics, Inc., 2013.

[3] S. P. Jones and J. D. DeLaurier. Aerodynamic estimation techniques for aerostats and airships. *Journal of Aircraft*, 20(2):120–126, 1982.

[4] B. Kämpf. *Flugmechanik und Flugregelung von Luftschiffen*. PhD thesis, University of Stuttgart, 2004.

[5] A. Kornienko. *System identification approach for determining flight dynamical characteristics of an airship from flight data*. PhD thesis, University of Stuttgart, 2006.

[6] M. M. Munk. The aerodynamic forces on airship hulls. Technical report, NACA, 1926. National Advisory Committee for Aeronautics, Report No.184.

[7] C. E. D. Riboldi, M. Belan, S. Cacciola, R. Terenzi, S. Trovato, D. Usuelli, and G. Familiari. Preliminary sizing of a low-altitude airship including ion-plasma thrusters. In *34th Congress of the International Council of the Aeronautical Sciences (ICAS2024), 9-13 September 2024, Florence, Italy*, 2024.

[8] C. E. D. Riboldi and A. Rolando. Layout Analysis and Optimization of Airships with Thrust-Based Stability Augmentation. *Aerospace*, 9:393, 2022.

[9] C. E. D. Riboldi and A. Rolando. Autonomous flight in near hover and hover for thrust controlled unmanned airships. *Drones*, 7, 2023.

[10] C. E. D. Riboldi and A. Rolando. Thrust-based stabilization and guidance for airships without thrust-vectoring. *Aerospace*, 10, 2023.

[11] C. E. D. Riboldi, A. Rolando, S. Cacciola, G. Regazzoni, and I. Spadafora. On the Optimal Preliminary Design of High-Altitude Airships: Automated Procedure and the Effect of Constraints. In *Aerospace Europe Conference 2023 - 10th EUCASS - 9th CEAS, 9-13 July 2023, Lausanne, Switzerland*, 2023.

[12] C. E. D. Riboldi, A. Rolando, and G. Regazzoni. On the feasibility of a launcher-deployable high-altitude airship: Effects of design constraints in an optimal sizing framework. *Aerospace*, 9:1–37, 2022.

[13] C. E. D. Riboldi and M. Tomasoni. Formation Flight of Fixed-Wing UAVs: Dynamic Modeling, Guidance Design, and Testing in Realistic Scenarios. *Aerospace*, 12:260, 2025.

[14] L. Trainelli, C. E. D. Riboldi, A. Rolando, and F. Salucci. Methodologies for the initial design studies of an innovative community-friendly miniliner. In *IOP Conference Series: Materials Science and Engineering*, volume 1024, 2021.